Hindawi
Geofluids
Volume 2021, Article ID 1968846, 13 pages
https://doi.org/10.1155/2021/1968846

Research Article

Influence of Mine Earthquake Disturbance on the Principal Stress of the Main Roadway near the Goaf and Its Prevention and Control Measures

Penghui Guo,[1] **Jiazhuo Li**,[1,2,3] **Xiqing Hao**,[4] **Heng Cui**,[5] **Lihua Tian**,[4] **Wenhao Xie**,[1] **and Jiaqi Chu**[1]

[1]*School of Mining Engineering, Anhui University of Science and Technology, Huainan, Anhui 232001, China*
[2]*Institute of Energy, Hefei Comprehensive National Science Center, Hefei, Anhui 230031, China*
[3]*School of Mining Engineering, China University of Mining and Technology, Xuzhou 221116, China*
[4]*Gaozhuang Coal Industry Co., Ltd., Zaozhuang Mining Group, Jining, Shandong 277605, China*
[5]*Shandong Energy Zikuang Group, Zibo, Shandong 250014, China*

Correspondence should be addressed to Penghui Guo; gph1996@yeah.net and Jiazhuo Li; jiazhuoli@aust.edu.cn

Received 4 August 2021; Accepted 7 September 2021; Published 16 September 2021

Academic Editor: Bailu Teng

With the reduction and depletion of shallow energy, the mining depth of coal around the world is increasing year by year, and the mining depth of some coal mines in China has reached kilometers. The main roadway near the goaf with the deep high static stress is very easy to be damaged after being disturbed by the mine earthquake. Taking the main roadway in the no. 1 mining area of Gaojiapu coal mine in Binchang mining area, Shaanxi Province, China, as the engineering background, the high-energy mine earthquake monitored by the on-site microseism is equivalently simulated through the dynamic module of FLAC^{3D}, and the spatial-temporal rotation characteristics of the principal stress of roadway surrounding rock under the disturbance of mine earthquake are studied and analyzed and put forward corresponding prevention and control measures. Research shows early stage of mine earthquake disturbance, roadway roof is first affected, and the principal stress of the roof has the trend of deflection to the side of the goaf. In the middle stage of mine earthquake disturbance, the main body of roof principal stress deflects to the side of goaf, and the deflection range is large. In the later stage of mine earthquake disturbance, the principal stress directions in the surrounding rock reverse rotation, and the reverse rotation angle of the principal stress direction in the roof is the largest. Finally, the asymmetric distribution characteristics of principal stress rotation are verified by using the asymmetric deformation phenomenon on both sides of roadway surrounding rock. Based on the rotation characteristics of principal stress under the dual influence of mine earthquake disturbance and goaf, optimize the layout scheme and blasting parameters of blasting pressure relief holes. The transmission direction of principal stress can be changed by blasting pressure relief method; meanwhile, the transmission of principal stress can be blocked; through the comparison of microseismic activity law before and after pressure relief, pressure relief effect is good. The research results can provide a certain reference basis for coal mine roadway pressure relief and reducing disaster conditions.

1. Introduction

Energy and mineral resources are important factors restricting the national economic development of all countries in the world; with the reduction and depletion of shallow resources, the mining depth of coal all over the world is increasing year by year [1–3]. At present, the mining depth of coal mines in China is increasing at the rate of 8~12 m per year; the eastern mine develops at the rate of 100~250 m every ten years; it is estimated that in the next twenty years, many coal mines will enter a depth of 1000~1500 m. With the excavation and construction of

underground space entering the deep mining, geological environment has become more complex; it makes the rock mechanics of deep underground engineering become the focus of international research in the field of mining and rock mechanics [4, 5].

After entering deep mining, while bearing high in situ stress, the rock mass experiences strong mining disturbance, and mining disturbance often induces seismicity, which is called mine earthquake [6–9]. With the increase of coal mining depth, underground coal mines are gradually affected by mine earthquakes [10, 11]. Under deep in situ stress, tectonic stress, and engineering disturbance, it causes the whole coal rock system to lose structural stability; engineering disasters such as large deformation failure, collapse, and rock burst occur in the surrounding rock; it not only affects the progress of the whole project but also threatens the life safety of construction personnel [12, 13].

Many scholars have studied the deformation and failure of roadway surrounding rock and its stress field environment. Yang et al. [14] studied the stability of roadway surrounding rock under dynamic disturbance (stress time curve) by using orthogonal test method. Chen et al. [15] believe that mining disturbance changes the size and direction of stress field in roadway surrounding rock, which is the main factor for asymmetric deformation of roadway. Xu et al. [16] studied the stress environment of lower coal seam roadway with the principal stress difference as the measurement index. Yang et al. [17] studied the frequency spectrum characteristics of rockburst vibration wave and the failure law of roadway surrounding rock by using the similar simulation experiment method. Li et al. [18] studied the action of principal stress in different directions by model test and numerical simulation, damage, and failure law of surrounding rock of straight wall arch tunnel. Xie et al. [19] used FLAC^{3D} to simulate the principal stress difference of roadway surrounding rock, the response characteristics of plastic zone, and the evolution law of two groups of principal stress difference under the condition of buried depth of 550~1250 m. Niu et al. [20] with the help of self-developed three-dimensional stress testing elements reveal the true loading and unloading stress path of surrounding rock at different depths of deep roadway and the stress state before and after excavation; the evolution law of the principal stress difference of surrounding rock inside and outside the loose zone is mainly analyzed, and combined with the failure range and mode of surrounding rock, its mechanism is discussed. Li et al. [21] studied the variation law of the direction of the principal stress field of the surrounding rock on the side of the goaf and its influence mechanism on the distribution of plastic zone of surrounding rock along goaf roadway; the mechanism of nonuniform large deformation of deep goaf roadway is revealed. Underground rock mass engineering is usually in a complex triaxial stress state; before the rock mass is excavated, the primary rock stress is in equilibrium. The original stress balance state is destroyed when excavating roadway or mining; under the influence of mining disturbance, the stress in the rock mass is redistributed; extending from the excavation boundary to the interior of surrounding rock, the stress field gradually returns to the original rock equilibrium state [22–24]. The excavation and construction of underground space engineering will not only change the near-field stress of disturbed surrounding rock but also change the direction of stress [25–28]. A large number of geotechnical experiments show that principal stress rotation is a mechanical problem that must be considered in geotechnical engineering [29–31].

Therefore, this paper takes the principal stress closely related to the deformation and failure of rock mass as the starting point; the spatial-temporal rotation law of principal stress direction under mine earthquake disturbance is expounded and put forward effective prevention and control measures; conclusion is verified by the deformation of roadway surrounding rock on-site, and the effect of prevention and control measures is tested by means of on-site microseismic monitoring. The research results can provide a certain reference basis for coal mine roadway pressure relief and reducing disaster conditions.

2. Engineering Geological Background

Gaojiapu coal mine is located in the northwestern part of the Binchang mining area in Shaanxi Province, China; it is the second pair of modern large-scale mines developed and constructed by Shandong Energy Zikuang Group in Binchang mining area, Shaanxi Province. Gaojiapu well field connects with Yangjiaping and Mengcun well fields in the south, extends to the Jinghe River in the north, adjoins Yadian mine in the east, and extends to the border between Shaanxi and Gansu in the west. It is the administrative division of Gaojiapu well field under the jurisdiction of Changwu County in Shaanxi Province, 13 km away from Changwu County; it covers an area of 37.33 hm^2. The east-to-west length is approximately 25.7 km, and the south-to-north width is approximately 16.6 km; the field area is 219.1699 km^2, the geological resource reserves are 970 million tons, and the designed recoverable resource reserve is 470 million tons. The design production capacity of Gaojiapu mine is 5.0 Mt/a, and the service life is 62.5 years; in this mine, 4# coal seam of Jurassic Yanan formation is mainly exploited, and the average burial depth is 960 m; the average thickness of the 4# coal seam in no. 1 mining area is 10 m. The geographical location of Gaojiapu coal mine and the distribution map of surrounding mines are shown in Figure 1.

The main coal roadway in no.1 mining area of Gaojiapu coal mine is located at 4# coal seam, the roadway section shape is straight wall semicircular arch, roadway is 5.8 m wide, the wall is 3 m high, and the arch is 3 m high. The right side of the main roadway is the goaf (three working faces on the right have been mined); use the underground elevation data of the no. 1 mining area of the coal seam to draw the surrounding environment and topographic map of the main roadway (as shown in Figure 2). It can be clearly seen that the main roadway is in the syncline axis; therefore, it is seriously affected by strong tectonic stress.

Figure 1: Geographical location of Gaojiapu coal mine and its surrounding coal mine distribution.

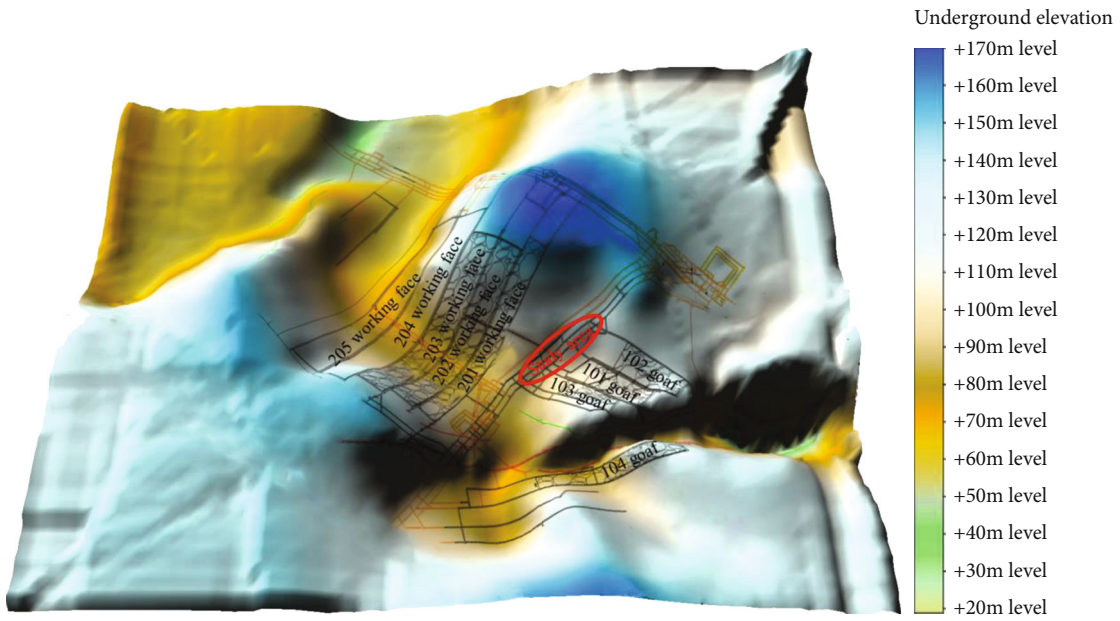

Figure 2: Surrounding environment and terrain of main roadway.

3. Research Methods

3.1. On-Site Mine Earthquake Monitoring. Microseismic monitoring technology is to utilize the microearthquake phenomenon in the process of coal rock mass failure. The seismic wave generated by the internal fracture of coal mass is monitored in real time by setting up microseismic monitoring probe in three-dimensional space around the coal rock mass. Various vibration parameters (vibration energy, vibration frequency, vibration torque, pressure drop, etc.) are determined through the analysis of microseismic events and focal location; on this basis, the stress state and failure of coal and rock mass are judged. Microseismic monitoring technology is considered as the most potential monitoring method for deformation and instability of coal and rock mass [32].

Import the waveform file monitored by the pickup in the microseismic system into the microseismic 3D visualization software (independently developed by Linming Dou team of China University of Mining and Technology), delineate the main roadway area of no. 1 mining area through geological coordinates, and export the data of mine earthquake events in the area, including mine earthquake frequency, energy level, and other information. Then, locate the exported mine seismic data into the mine geological CAD map; the position of the mine shock in the vertical direction can be obtained from the profile chart. On the day of an accident in the main roadway of no. 1 mining area of Gaojiapu coal mine, two large energy events of 10^5~106 J were detected in the area of 20 meters above the roof; the location distribution of mine earthquake focal points is shown in Figure 3.

3.2. Numerical Simulation

3.2.1. Establishment of Numerical Model. Taking the main coal roadway in no. 1 mining area of Gaojiapu coal mine as the simulation object, the numerical model is established by using FLAC^{3D} software; model size is 520 m × 400 m × 100 m, and the model is established as shown in Figure 4. According to the in situ stress measurement report on the mine, the ratio of the maximum horizontal principal stress to the minimum horizontal principal stress is 4.48~5.25, and maximum horizontal principal stress is about 1.61~1.81 times of the vertical principal stress. The in situ stress field is dominated by horizontal stress, it belongs to high-level tectonic stress field; therefore, the influence of principal stress on roadway surrounding rock is mainly considered. The values of physical and mechanical parameters of surrounding rock in the model are listed in Table 1, the Mohr-Coulumb failure criterion was adopted, and the boundary conditions were determined as follows:

(1) The displacement boundary constraint was applied to the model perimeter. The velocities in the x direction at the left and right boundaries, in the y direction at front and rear boundaries, and those in the x, y, and z directions at the bottom boundary were zero

(2) The upper boundary of this model was a free boundary, and a vertical uniformly distributed load was applied to simulate the self-weight load of overlying strata. Given the influence of self-weight of this model, the self-weight load of overlying strata applied was 22.5 MPa

(3) The geostatic stress field was applied to this model, and the gravitational acceleration was taken as 9.81 m/s^2

(4) The average value of lateral pressure coefficient is 1.7; the applied value of lateral stress is 1.7 times of overburden self-weight stress

Because the research object is the main coal roadway in no. 1 mining area, one working face is excavated at one time; as the 104 goaf is far from the main roadway, only three working faces are excavated to simulate the goaf on one side of the main roadway; according to the actual mining sequence of Gaojiapu coal mine, three working faces are excavated in turn and calculated to balance.

3.2.2. Application of Dynamic Load Disturbance. Reference [33] obtained the waveform characteristics of roof fracture and fault activation events through microseismic monitoring; according to the elastic wave theory, any complex stress wave can be obtained by Fourier transform of several simple harmonic waves, that is, simple harmonic is the basic form of downhole complex stress wave. According to reference [34], the duration of vibration recorded by the microseismic monitoring system is only tens of milliseconds when rock burst occurs on-site; generally, there is no effect of multiple rounds of impact in the dynamic load source of rock burst. If the mine earthquake wave is simplified into simple harmonic, the main frequency of mine earthquake is about 10~20 Hz, and the period is 0.05~0.1 s; when the dynamic load time applied in the simulation is about one period, the coal and rock mass will be destroyed. Therefore, the dynamic module in FLAC^{3D} software is used to apply a sinusoidal stress wave 20 m above the roadway to simulate mine earthquake and set the source strength of 48 MPa (equivalent to 10^6 J energy) [35] and frequency of 20 Hz; the action time of dynamic load is 0.1 s, and the dynamic load waveform is shown in Figure 5

3.2.3. Study the Principal Stress Direction through the Equal Angle Stereonet. There is a process of damage development in the failure of coal and rock mass; under the action of stress, there is a certain speed of crack propagation; it takes a certain time for microcracks to propagate from micro to penetration and nucleation to form macrofracture surface. Therefore, under the action of dynamic load, before coal failure, the stress can increase to a higher value in a period of time, showing high strength. On the contrary, inside the coal body, when the superposition of dynamic load and static load makes the principal stress axis rotate, the crack that is not easy to expand under static load can expand and aggravate the damage of coal and rock mass. The damaged coal and rock mass forms a stacked block structure, and its strength has various anisotropy, the principal stress direction rotates under dynamic load, and instability probability of block structure is increased.

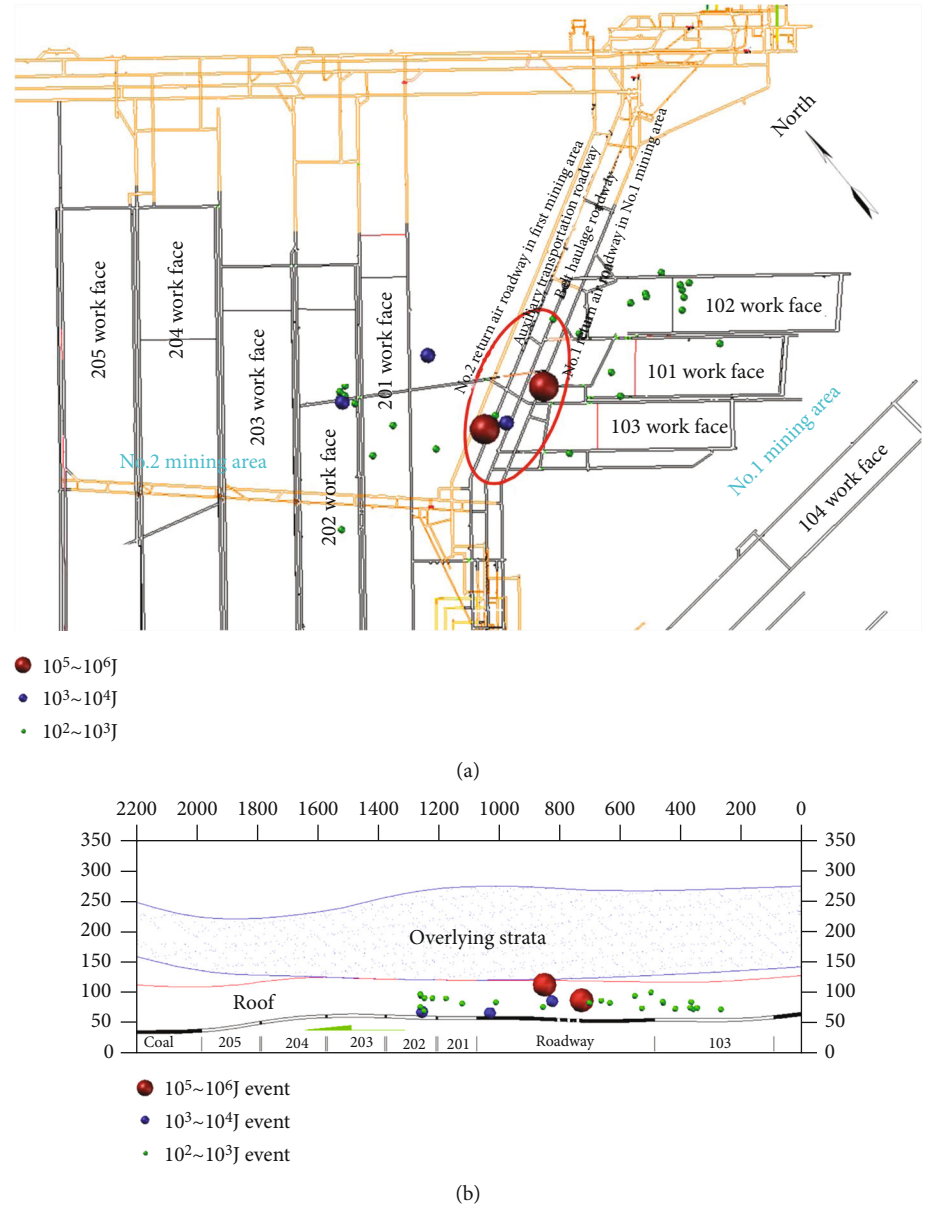

Figure 3: Location distribution of mine earthquake sources monitored by microseism. (a) Plane distribution of mine earthquake; (b) profile distribution of mine earthquake.

Under dynamic load, coal and rock masses show the characteristics of microdamage, decrease of critical static load stress, and increase of macrofailure strength. When the dynamic load fluctuates in the state of "increase-decrease-increase-decrease," the microdamage continues, the macrostress does not increase to the maximum, and coal and rock mass shows damage fatigue failure. Therefore, coal and rock masses are more likely to be damaged under dynamic load. The large-scale coal body contains a large number of joints and fractures. The randomly distributed primary fractures may be formed in the coal forming process or in the later tectonic movement. The existence of fractures leads to the anisotropic mechanical characteristics of coal, that is, the mechanical behavior of coal will change due to the rotation of the direction of principal stress.

Because the three-dimensional principal stress direction is a spatial vector, the evolution law of the principal stress direction of surrounding rock in the mining process cannot be described intuitively and accurately on the plane. Therefore, this paper uses the equal angle stereonet in geological data processing to represent the variation law of azimuth and inclination angle in the direction of principal stress [36].

The equal angle stereonet is composed of a base circle and longitude and latitude grid; the base circle is the stereographic equatorial large circle of the projection sphere, and the longitude and latitude grid is composed of a series of large longitudinal arcs and a series of small latitudinal arcs. The geometric elements (lines and planes) of the three-dimensional space of the object are reflected on the projection plane for research and processing, the spatial plane is

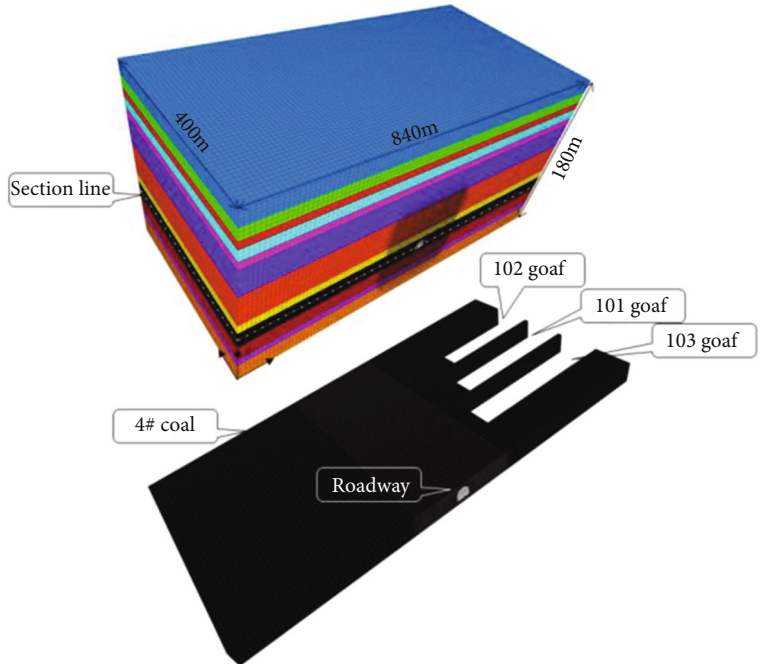

Figure 4: Numerical model of main roadway near goaf in no. 1 mining area of Gaojiapu coal mine.

Table 1: Physical and mechanical parameters of surrounding rock.

Rock formation	Bulk modulus (GPa)	Shear modulus (GPa)	Density (kg·m^{-3})	Cohesion (MPa)	Internal friction angle (°)	Uniaxial tensile strength (MPa)
Mudstone	6.08	3.47	2 480	1.2	30	0.61
Silty sandstone	10.8	8.13	2 460	2.75	38	2.67
Coarse sandstone	12	8	2 700	2.0	45	0.2
Silty sandstone	10.8	8.13	2 460	2.75	38	2.67
Coarse sandstone	12	8	2 700	2.0	45	0.2
Silty sandstone	10.8	8.13	2 460	2.75	38	2.67
Coarse sandstone	12	8	2 700	2.0	45	0.2
Silty sandstone	10.8	8.13	2 460	2.75	38	2.67
4# coal	4.9	2.01	1 380	1.25	32	0.15
Mudstone	6.08	3.47	2 480	1.2	30	0.61
Coarse sandstone	12	8	2 700	2.0	45	0.2
Medium sandstone	11	8.5	2 820	3.2	42	1.29

displayed as an arc on the equal angle stereonet, and spatial straight line is displayed as a point on the equal angle stereonet; position of spatial plane and spatial line is represented by inclination angle/azimuth. The equal angle stereonet is not only a simple and intuitive calculation method, but also an image and comprehensive quantitative graphic method.

The principal stress direction of surrounding rock is a vector, so the inclination angle/azimuth is used to represent the position of this space vector. The inclination angle is defined as the acute angle between the main stress direction and its projection on the xy plane. Variation range of the inclination angle is -90°~90°, a positive value indicates that the principal stress direction is above the xy plane, and a negative value indicates that the principal stress direction is below the xy plane. The azimuth is defined as the angle between the clockwise rotation from the positive direction of the y-axis to the projection line of the principal stress direction on the xy plane; variation range of the azimuth is 0°~360°.

As shown in Figure 6, on the equal angle stereonet, the projection of the principal stress direction is a point; by

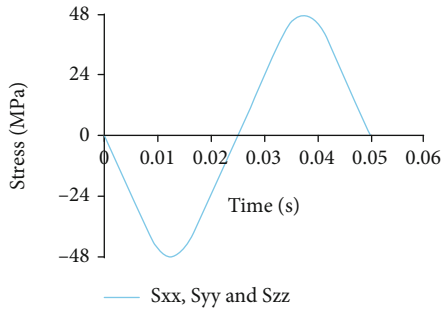

Figure 5: Dynamic stress waveform.

connecting the center of the equal angle stereonet with the projection point and extending it to intersect the equatorial large circle, the reading at the intersection is the azimuth. Rotate the connected straight line to the horizontal along the direction of the acute angle with the horizontal straight line, and the indication of the projection point in the direction of the principal stress at the position on the horizontal straight line is the inclination angle.

4. Result Discussion

4.1. Spatial-Temporal Rotation Characteristics of Principal Stress. Figure 7 shows the equal angle stereonet of the principal stress direction of the surrounding rock of the deep roadway with the action time of the dynamic load.

As can be seen from Figure 7, before dynamic load disturbance, due to the dual influence of high-level tectonic stress and excavation unloading effect, the direction of principal stress in surrounding rock deviates from xy plane (recorded as horizontal plane), but still in a vertical plane parallel to the x-axis (recorded as plane α).

When the dynamic load disturbance is 0.01 s, the dynamic load stress wave does not propagate to the coal seam, so there is no obvious change in the direction of principal stress in the coal seam and floor. The main azimuth of the principal stress in the roof is inclined to the side of the roadway goaf, between 30° and 90°. The inclination angle decreases, between 45° and 90°, deviate from the vertical plane parallel to the y-axis (recorded as plane β).

During dynamic load disturbance of 0.03 s~0.05 s, the azimuth of the roof varies greatly, and the inclination angle is between 45° and 75°. As the dynamic load disturbance stress wave propagates to the roadway floor, the inclination angle of the main stress of the coal seam deflects towards the horizontal plane; the inclination angle and azimuth are reduced; by plane α, directional plane β rotates; the rotation amplitude is close to 90°. The azimuth of the principal stress of the floor does not change obviously, and the inclination angle decreases slightly, but the main body is still inside plane α.

When dynamic load disturbance is 0.07 s~0.09 s, the principal stress of disturbed surrounding rock rotates reversely, the principal stress of the roof faces plane β deflection, and the inclination angle increases obviously. The principal stress of the coal seam deviates from the horizontal plane, the inclination angle and azimuth increase, and by plane β, directional plane α rotates. There is no obvious reverse rotation in the main stress direction of the floor.

4.2. On-Site Investigation. At present, there is no effective monitoring method for the rotation characteristics of principal stress; however, according to the deformation characteristics of surrounding rock, the rotation characteristics of the principal stress direction can be qualitatively analyzed, and the destruction scene of the main roadway in no. 1 mining area of Gaojiapu coal mine is shown in Figure 8.

There are obvious differences in the deformation characteristics of surrounding rock on both sides of the main roadway, the deformation of surrounding rock on the coal side of the roadway is small, and it is mainly horizontal displacement. The deformation of surrounding rock at the side of roadway goaf is large, and the displacement direction has a certain included angle with the horizontal plane; the vertical spatial relationship between the roadway side and the horizontal plane is no longer maintained, and the included angle between the two is reduced to 70°. In Figure 8, the asymmetric characteristics of surrounding rock deformation of roadways on both sides of the working face are caused by the rotation difference in the direction of principal stress. The surrounding rock at the coal side of the roadway is less affected by mining, and the concentration of principal stress is low; the rotation range of principal stress is small, and the failure range of surrounding rock is small. Its deformation is mainly due to the compression effect of high-level tectonic stress, mainly horizontal deformation. The surrounding rock at the side of roadway goaf is highly affected by mining, and the concentration degree of principal stress is high; the rotation range of principal stress is large, and the failure range of surrounding rock is large. Its deformation is mainly due to the plastic flow of roadway surrounding rock caused by the deflection of principal stress.

4.3. Influence of Mine Earthquake Disturbance. The goaf is on the right side of the main roadway in no. 1 mining area of Gaojiapu coal mine (as shown in Figure 9). According to the masonry beam theory, after the main roof is broken, an arc triangular plate "b" is formed at both ends of the working face, and a trapezoidal plate "a" is formed in the middle of the working face. Under the support of solid coal, coal pillar, and goaf gangue, the arc triangular plate and trapezoidal plate form a lateral masonry beam structure along the inclined direction of the working face. The rotation of the rock block on the main roof of the fault forms a strong horizontal extrusion force; it is possible to form a three-hinged arch balance structure under the action of mutual extrusion; the stability of this equilibrium structure will depend on whether the extrusion force at the bite point exceeds the strength limit at the contact surface of the bite point. In this case, as long as the total stress (superposition of static stress and dynamic stress) on the rock block contact surface exceeds the strength limit ($[\sigma]$) at the end of the rock block, it can lead to the rotation of the "masonry beam" structure of the main roof and then deformation and instability.

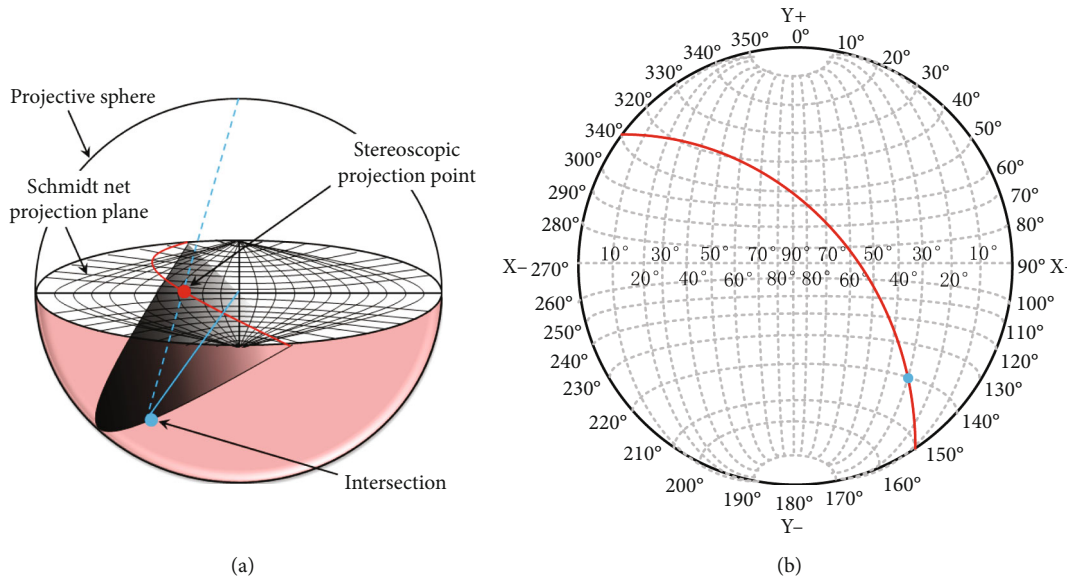

Figure 6: The equal angle stereonet.

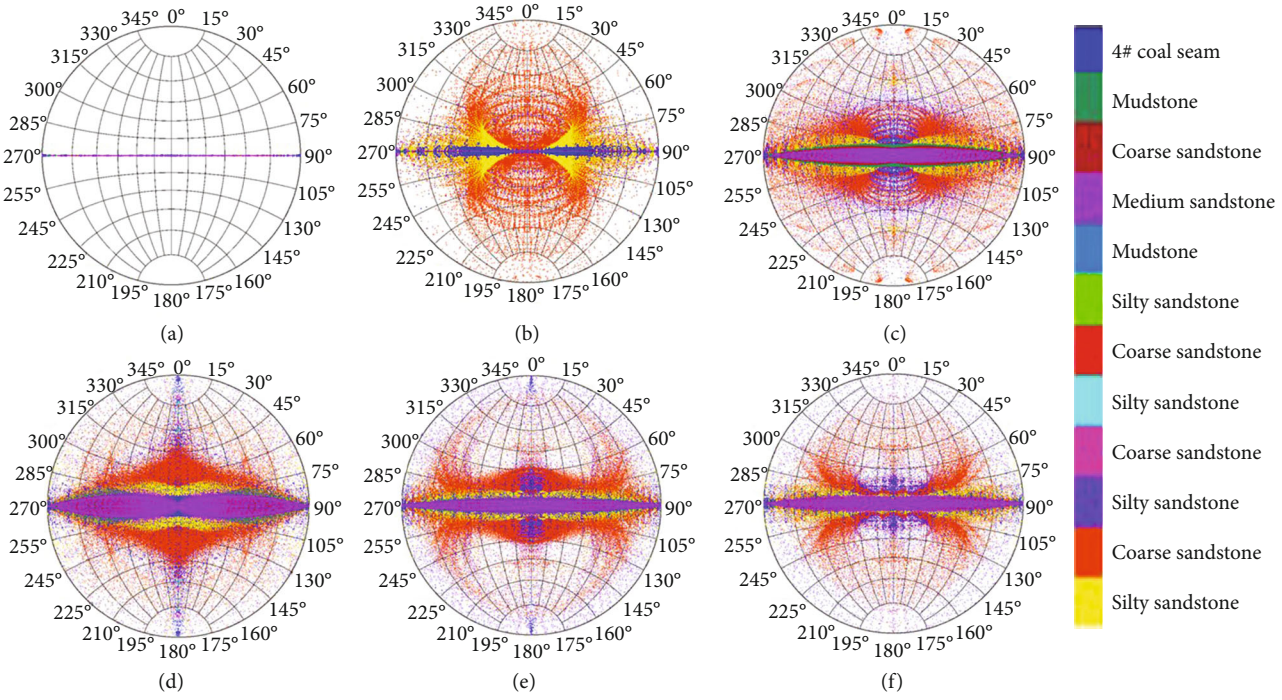

Figure 7: Evolution track of principal stress direction under dynamic load disturbance. (a) Before dynamic load disturbance; (b) dynamic load disturbance 0.01 s; (c) dynamic load disturbance 0.03 s; (d) dynamic load disturbance 0.05 s; (e) dynamic load disturbance 0.07 s; (f) dynamic load disturbance 0.09 s.

Under the disturbance of mine earthquake, the rotation angle of arc triangular "b" increases, the principal stress direction rotates, eventually loses stability, and slides to the goaf. The principal stress distribution in the top coal on the right side of the green dotted line is always affected by the rotation position of the arc triangular plate "b." The force (F) of mine earthquake disturbance stress wave, arc triangular plate, and overburden collapse rock block on direct roof and lower coal seam, perpendicular to the contact surface between the direct roof and the triangular plate. During the rotation and sinking of the arc triangular plate "b," the direction of the contact surface also changes; therefore, the magnitude and direction of the pressure (F) are related to the rotation angle (θ) of the arc triangle. With the change of the magnitude and direction of roof pressure (F), the stress boundary conditions of direct roof and coal seam

Figure 8: Main roadway destruction site.

change, and it will inevitably affect the magnitude and direction of principal stress in roadway surrounding rock.

5. Pressure Relief Measures

5.1. Optimization of Relevant Parameters for Blasting Pressure Relief. After the roadway is excavated, a free space is formed in the rock mass; it provides space for the deformation of floor rock. The root cause of roadway floor heave are as follows: the vertical stress on the roof is transmitted to the two sides, causing two sides to sink; the sinking of the two sides caused the destruction of the two bottom corners; sinking of the two sides caused the failure of the two bottom corners; floor is squeezed by the secondary horizontal principal stress; the roadway floor expands into the roadway and finally shows floor heave deformation. The problem of floor heave in roadway under high stress environment becomes particularly prominent, high stress leads to the increase of the pressure on the roof and floor of the coal seam, and the clamping effect on the coal seam is more obvious; as the fluidity (ductility) of the coal body increases, the floor heave caused by the subsidence of the two sides will be more serious.

Based on the previous blasting parameters of Gaojiapu coal mine, the blasting construction technical requirements are as follows:

(i) Materials and tools required for blasting construction: $\Phi 60 \times 440 \times 1$ mm blasting cartridge, mine grade III emulsion explosive, synchronous millisecond delay electric detonator, blasting mud, cement, grouting pipe, return pipe, hemp, detonator, detonating cord, blasting busbar, gun rod, insulating tape, etc.; the schematic diagram of blasting hole charging is shown in Figure 10

(ii) Blasting method: FG-500A detonator is used for initiation; millisecond detonate is used for group blasting and single hole detonate

(iii) Blasting parameters and blasting operation process:

(1) Using a blasting cartridge as a carrier for explosives, charge 20 kg

(2) The charging method is positive continuous charging and slowly sent to the hole bottom

(3) Before charging, the residual coal and rock powder in the borehole must be removed. Use PVC gun rod to detect the actual depth of drilling hole and confirm that the drilling depth is normal and meets the requirements of measures; charging can be carried out only after there is no residual coal and rock powder

(4) An operation platform shall be set up before charging, and a 1.2 m high protective fence shall be welded around the platform with waste anchor bolts

(5) Before charging, cut off the blasting barrel at one end of the explosive with a saw blade; one 80 mm long steel wire shall be crossed on both sides of the blasting barrel to prevent the explosive from sliding naturally in the borehole

(6) Index the detonator to the orifice position and then seal the hole (during grouting and hole sealing, the grouting pipe shall be fixed with hemp and blasting mud, and a 0.5 m hole section shall be reserved at the orifice)

(7) When blasting, two detonating cords are connected in parallel with two-millisecond delay electric detonators with the same number at the orifice, seal the joint between detonator and detonating cord with insulating tape, install the detonator and detonating cord, leave a distance of 0.5 m, and then, seal the hole with sealing agent

5.2. Principle of Blasting Pressure Relief. Under the disturbance of mine earthquake, the main stress of roadway surrounding rock deflects to the side of the goaf to form a stress concentration area; the side roof and floor near the goaf of the roadway are seriously damaged. In view of the above problems of roof subsidence and floor heave, the purpose of blasting pressure relief in the roof and floor of the roadway is to reduce the stress concentration, block the transmission of the principal stress in the roof and floor, and reduce the impact of the deflection of the principal stress. The diameter of roof blasting hole is 75 mm, the distance between holes is 5 m, the depth of blasting hole is 40 m, the drilling inclination angle is 60°, and the charge is 20 kg. The diameter of the bottom plate blasting hole is 75 mm, the spacing between holes is 1 m, and the depth of the blasting hole is 12 m until the rock is seen on the floor of the coal seam; the drilling inclination angle is 60°, the charge is 10 kg, and the final hole position of the blasting hole is determined at the peak stress of the floor.

The essence of blasting pressure relief is continuous blasting of multiple blasting holes, and each blasting hole adopts two millisecond detonators; group blasting and single hole detonate create a free surface for the next stage of blasting and make the blasting crack develop in the set direction. By controlling the propagation direction of detonation wave, a continuous weak structural plane is formed in the rock

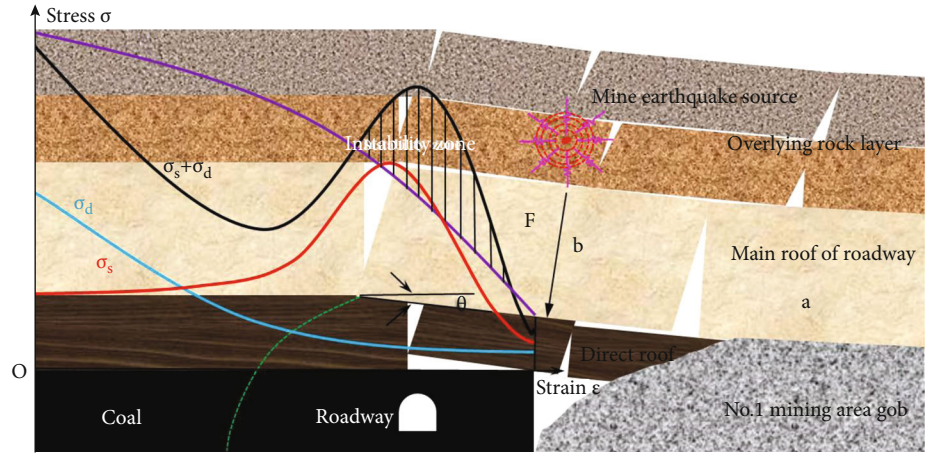

Figure 9: Structure of the side roof in the goaf of main roadway.

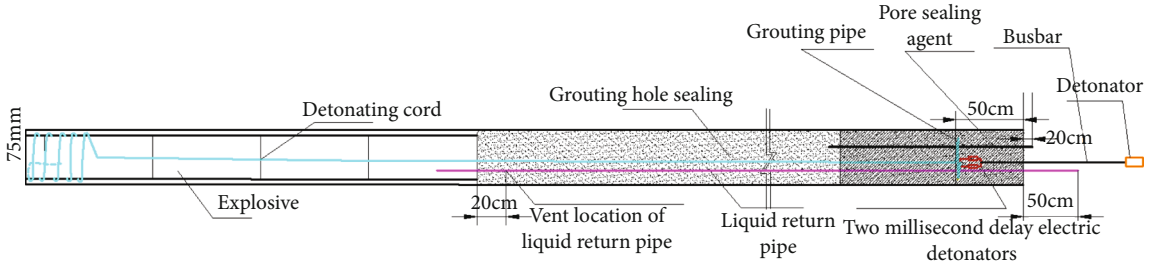

Figure 10: Schematic diagram of blasting hole charging.

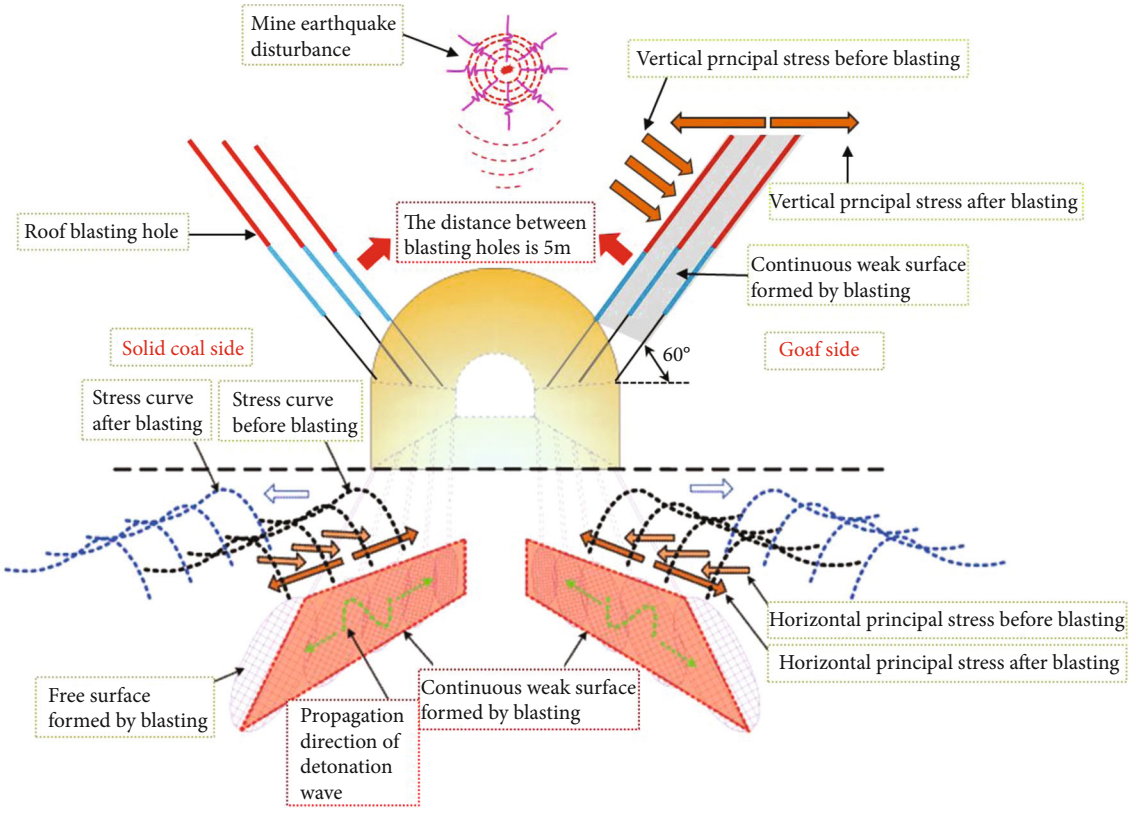

Figure 11: Blasting blocking stress transmission.

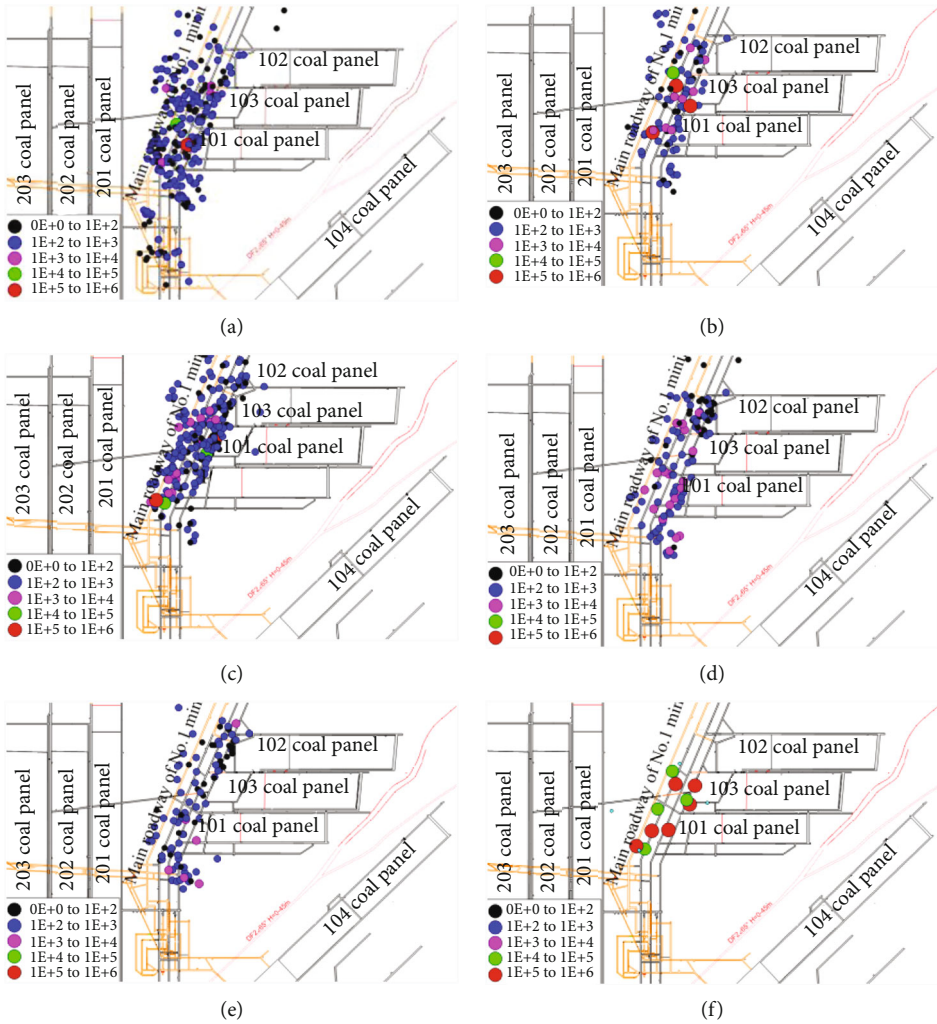

Figure 12: Plane distribution of microseismic events before and after prevention and control of main roadway. (a) August 2017; (b) September 2017; (c) October 2017; (d) November 2017; (e) December 2017; (f) August to December 2017.

layer of roof and floor. The existence of structural plane can change the transmission direction of principal stress so that the principal stress does not deflect to the side of roadway goaf. At the same time, it blocks the transmission of principal stress to the goaf side and floor of the roadway, reduce the horizontal extrusion force on the floor coal and rock mass, and control the serious deformation and floor heave of the goaf side of the roadway (as shown in Figure 11).

5.3. Pressure Relief Effect Test. Microseismic activity can reflect the fracture of coal and rock mass; therefore, the roadway pressure relief effect can be roughly determined based on the change of high-energy microseismic events with time; the significant reduction of high energy events indicates that the pressure relief effect is good.

The main roadway area is selected as the statistical area; after the above blasting scheme is adopted for construction, the prevention and control effect is evaluated through microseismic monitoring. Since the construction protection is carried out in October 2017, August and September 2017 are selected for comparison with November and December 2017; a total of four months are used as the time period for comparison before and after the implementation of pressure relief measures; the plane distribution of microseismic events at this stage is shown in Figure 12.

As can be seen from Figure 12, before the implementation of pressure relief measures (August~September), the total energy of microseismic is larger, and the large energy microseismic events (greater than 10^5 J) are more. During the implementation of pressure relief measures (October), the total number of microseismic events and large energy microseismic events are too many due to the disturbance caused by construction. After the implementation of pressure relief measures (November~December), the total number of microseismic events decreased slightly, it shows that the adopted pressure relief scheme transfers part of the elastic energy stored in coal and rock mass to the deep. There are no large energy microseismic events; it shows that the adopted pressure relief scheme releases the elastic energy stored in coal and rock mass; elastic energy is mostly released in the form of small energy microseismic events (less than 10^4 J); thus, the degree of stress concentration is reduced.

6. Conclusions

The main roadway near the goaf with the deep high static stress is very easy to be damaged after being disturbed by the mine earthquake. Taking the main coal roadway of no. 1 mining area of Gaojiapu coal mine as the engineering background, through numerical simulation and field monitoring methods, the spatial-temporal rotation characteristics of the principal stress of roadway surrounding rock under the disturbance of mine earthquake are studied and analyzed and put forward corresponding prevention and control measures. The research results can provide a certain reference basis for coal mine roadway pressure relief and reducing disaster conditions. The main conclusions of this paper are summarized as follows:

(1) In the early stage of mine earthquake disturbance, the roadway roof is first affected, and the main stress of the roof tends to deflect to the side of the goaf. In the middle stage of mine earthquake disturbance, the main body of roof principal stress deflects to one side of goaf, and the deflection range is large. In the later stage of mine earthquake disturbance, the principal stress direction in the surrounding rock rotates reversely, and the rotation angle of the principal stress direction in the roof is the largest

(2) The asymmetric distribution characteristics of principal stress rotation are verified by using the asymmetric deformation phenomenon on two sides of roadway surrounding rock; based on the rotation characteristics of principal stress under the dual influence of mine earthquake disturbance and goaf, optimize the layout scheme of blasting pressure relief hole and blasting parameters. The transmission direction of principal stress can be changed by blasting; at the same time, it blocks the transmission of principal stress, through the comparison of microseismic activity law before and after pressure relief; the pressure relief effect is good

Data Availability

All data included in this study are available upon request from the corresponding author.

Conflicts of Interest

The authors declare that there are no conflicts of interest regarding the publication of this paper.

Acknowledgments

This research was supported by the National Natural Science Foundation of China (52004004) and China Postdoctoral Science Foundation of China (2019M661991).

References

[1] L. M. Xue, W. J. Zhang, Z. Zheng et al., "Measurement and influential factors of the efficiency of coal resources of China's provinces: based on Bootstrap-DEA and Tobit," *Energy*, vol. 221, no. 4, p. 119763, 2021.

[2] Y. Zhao, T. H. Yang, H. L. Liu et al., "A path for evaluating the mechanical response of rock masses based on deep mining-induced microseismic data: a case study," *Tunnelling and Underground Space Technology*, vol. 115, no. 5, 2021.

[3] T. Li, B. G. Yang, Z. Qi, C. J. Gu, Q. Y. Shan, and W. Chen, "Numerical simulation of roof movement and fill strength of coal deep mining," *Arabian Journal of Geosciences*, vol. 14, no. 8, 2021.

[4] M. C. He, X. J. Lv, and H. H. Jing, "Characters of surrounding rockmass in deep engineering and its non-linear dynamic-mechanical design concept," *Chinese Journal of Rock Mechanics and Engineering*, vol. 21, no. 8, pp. 1215–1224, 2002.

[5] M. C. He, H. P. Xie, S. P. Peng, and Y. D. Jiang, "Study on rock mechanicsin deep mining engineering," *Chinese Journal of Rock Mechanics and Engineering*, vol. 24, no. 16, pp. 2803–2813, 2005.

[6] S. M. Hsiung, W. Blake, A. H. Chowdhury, and T. J. Williams, "Effects of mining-induced seismic events on a deep underground mine," *Pure and Applied Geophysics PAGEOPH*, vol. 139, no. 3-4, pp. 741–762, 1992.

[7] W. Kuhnt, P. Knoll, H. Grosser, and H. J. Behrens, "Seismological models for mining-induced seismic events," *Pure and Applied Geophysics PAGEOPH*, vol. 129, no. 3-4, pp. 513–521, 1989.

[8] J. A. Vallejos and S. D. McKinnon, "Correlations between mining and seismicity for re-entry protocol development," *International Journal of Rock Mechanics and Mining Sciences*, vol. 48, no. 4, pp. 616–625, 2011.

[9] W. Cai, L. M. Dou, G. Y. Si, and Y. W. Hu, "Fault-induced coal burst mechanism under mining-induced static and dynamic stresses," *Engineering*, vol. 7, no. 5, pp. 687–700, 2021.

[10] T. Li, M. F. Cai, and M. Cai, "A review of mining-induced seismicity in China," *International Journal of Rock Mechanics and Mining Sciences*, vol. 44, no. 8, pp. 1149–1171, 2007.

[11] W. J. Yu, B. Pan, F. Zhang, S. F. Yao, and F. F. Liu, "Deformation characteristics and determination of optimum supporting time of alteration rock mass in deep mine," *KSCE Journal of Civil Engineering*, vol. 23, no. 11, pp. 4921–4932, 2019.

[12] B. F. Wang, K. M. Sun, B. Liang, and H. B. Chi, "Experimental research on the mechanical character of deep mining rocks in THM coupling condition," *Energy Sources, Part A: Recovery, Utilization, and Environmental Effects*, vol. 43, no. 13, pp. 1660–1674, 2021.

[13] J. Z. Li, P. H. Guo, A. Y. Yuan, C. Q. Zhu, T. Zhang, and D. H. Chen, "Failure characteristics induced by unloading disturbance and corresponding mechanical mechanism of the coal-seam floor in deep mining," *Arabian Journal of Geosciences*, vol. 14, no. 12, 2021.

[14] Y. S. Yang, S. J. Wei, and D. M. Zhang, "Influence of rock burst and other disasters on stability of surrounding rock of roadway," *Geotechnical and Geological Engineering*, vol. 36, no. 3, pp. 1767–1777, 2018.

[15] S. Y. Chen, C. S. Song, Z. B. Guo, Y. Wang, and Y. Wang, "Asymmetric deformation mechanical mechanism and control countermeasure for deep roadway affected by mining," *Journal of China Coal Society*, vol. 41, no. 1, pp. 246–254, 2016.

[16] L. Xu, H. L. Zhang, D. K. Gen, and B. Li, "Principal stress difference evolution in floor under pillar and roadway layout,"

Journal of Mining & Safety Engineering, vol. 32, no. 3, pp. 478–484, 2015.

[17] Y. S. Yang, S. J. Wei, and S. N. Zhao, "Research on the destructional pattern of surrounding rock of roadway induced by dynamic disturbance," *Geotechnical and Geological Engineering*, vol. 37, no. 5, pp. 4447–4459, 2019.

[18] Y. X. Li, Z. M. Zhu, and J. L. Fan, "Effect of principal stress orientation on stability of surrounding rock of tunnels," *Chinese Journal of Geotechnical Engineering*, vol. 36, no. 10, pp. 1908–1914, 2014.

[19] S. R. Xie, S. J. Li, X. Huang, Y. Y. Sun, J. H. Yang, and S. X. Qiao, "Surrounding rock principal stress difference evolution law and control of gob-side entry driving in deep mine," *Journal of China Coal Society*, vol. 40, no. 10, pp. 2355–2360, 2015.

[20] S. J. Niu, H. W. Jing, and D. F. Yang, "Physical simulation study of principal stress difference evolution law of surrounding rock of deep mine roadways," *Chinese Journal of Rock Mechanics and Engineering*, vol. 31, no. S2, pp. 3811–3820, 2012.

[21] J. Li, N. J. Ma, and Z. W. Ding, "Heterogeneous large deformation mechanism based on change of principal stress direction in deep gob side entry and control," *Journal of Mining & Safety Engineering*, vol. 35, no. 4, pp. 670–676, 2018.

[22] S. Q. Yang, H. W. Jing, and Y. S. Li, *Experimental Investigation on Mechanical Behavior of Coarse Marble Under Six Different Loading Paths Springer US*, Springer US, 2011.

[23] H. P. Xie, H. W. Zhou, J. F. Liu et al., "Mining-induced mechanical behavior in coal seams under different mining layouts," *Journal of China Coal Society*, vol. 36, no. 7, pp. 1067–1074, 2011.

[24] M. G. Qian, P. W. Shi, and X. Z. Zou, *Mining Pressure and Strata Control*, China University of mining and Technology Press, 2003.

[25] Y. Q. Li, Z. M. Zhu, and R. Hu, "Study on the effect of principal stress orientation on tunnel stability," *Journal of Sichuan University(engineering science edition)*, vol. 44, no. S1, pp. 93–98, 2012.

[26] L. B. Guan, *Experimental Study on Effect of Principal Stress Axis Rotation on the Macro-Deformation and Microstructure of Intact Clay*, Zhejiang University, 2010.

[27] D. Jin, *Experimental Study on Effect of Rotation of Principal Stress Orientation on Saturated Sand*, Dalian University of Technology, 2009.

[28] Z. H. Wang, "Numerical simulation research on the influence of buried depth on the stress field of overlying rock in floor roadway," *IOP Conference Series: Earth and Environmental Science*, vol. 787, no. 1, p. 012129, 2021.

[29] M. Barla, "Numerical simulation of the swelling behaviour around tunnels based on special triaxial tests," *Tunnelling and Underground Space Technology*, vol. 23, no. 5, pp. 508–521, 2008.

[30] C. D. Chang and B. Haimson, "True triaxial strength and deformability of the German Continental Deep Drilling Program (KTB) deep hole amphibolite," *Journal of Geophysical Research: Solid Earth (1978–2012)*, vol. 105, no. B8, pp. 18999–19013, 2000.

[31] R. P. Tiwari, K. S. Rao, and R. Seshagiri, "Post failure behaviour of a rock mass under the influence of triaxial and true triaxial confinement," *Engineering Geology*, vol. 84, no. 3-4, pp. 112–129, 2006.

[32] H. He, L. M. Dou, and S. Y. Gong, "Induced impact of key strata in overlying strata," *Chinese Journal of Geotechnical Engineering*, vol. 32, no. 8, pp. 1260–1265, 2010.

[33] X. F. Xu, *Research of Mechanism and Controlling Technology of Floor Burst in Coal Seam Roadway*, China University of Mining and Technology, 2011.

[34] C. P. Lu, *Intensity Weakening Theory for Rockburst of Compound Coal-Rock and Its Application*, China University of Mining and Technology, 2008.

[35] A. N. Li, L. M. Ling, Z. Y. Wang, J. R. Cao, S. W. Wang, and C. H. Shan, "Numerical simulation of rock burst of horizontal sectional mining of near-vertical coal seam under dynamic load," *Coal Engineering*, vol. 50, no. 9, pp. 83–87, 2018.

[36] N. Duan, *Study on Mining-Induced Stress and Energy Evolution of Surrounding Rocks in Deep Mine*, China University of mining and technology, 2016.